

Synthesis, Characterization, and Thermal Studying of VO(II), Cu(II), Zn (II), Cd(II), and Au (III) Complexes with Azo Dye and Evaluation as Antioxidants

Areeg Malek Fadhel*¹  , Abbas Ali Salih Al-Hamdani²  , Wail Al Zoubi³  

¹Ministry of Education, Baghdad Education Directorate, Al-Rusafa II.

²Department of Chemistry, Collage of Science for Women, University of Baghdad, Baghdad, Iraq

³Materials Electrochemistry Group, School of Materials Science and Engineering, Yeungnam University, Gyeongsan, Republic of Korea

*Corresponding author.

Received 19/02/2024, Revised 20/05/2024, Accepted 22/05/2024, Published Online First 20/07/2024



© 2022 The Author(s). Published by College of Science for Women, University of Baghdad.

This is an open access article distributed under the terms of the [Creative Commons Attribution 4.0 International License](https://creativecommons.org/licenses/by/4.0/), which permits unrestricted use, distribution, and reproduction in any medium, provided the original work is properly cited.

Abstract

Complexes of Vanadyl, Copper, Zinc, Cadmium, and Aureate with their double valence and Aureate with its triple valence were prepared using the azo dye (2,4,6-trihydroxy-3-((3-hydroxyphenyl)dixenyl)phenyl)ethane-1-one prepared newly from diazonium salt With 2,4,6-trihydroxyacetophenone, after isolation. The prepared materials were identified by available spectroscopic methods and diagnostic techniques for C.H.N, IR, UV-Vis, ¹H&¹³C-NMR, Mass, thermogravimetric analysis curve, differential scanning calorimetry, and complexes, these techniques included as well as determining the metal percentage, determining the chlorine content, magnetic susceptibility, and molar conductivity. The results showed that the ligand is anionic (negative) tetradentate when coordinated with Vanadyl, Copper, Zinc, Cadmium through the phenolic oxygen atom, the carbonyl oxygen atom, and the azo nitrogen atom. It was tridentate e when it coordinated with Aureate through the phenolic oxygen atom and the azo nitrogen atom, giving the planar square shape (neutral) while the zinc and cadmium were (neutral) octahedral containing two coordinated water molecules and copper was tetrahedral shape (neutral) and Vanadyl complex give trigonal bipyramidal shape (neutral). Then the potential of these prepared compounds as antioxidants was determined by inhibiting free radicals using DPPH as a free radical and vitamin C as a reference to determine The Radical scavenging activities gave the results (Au-complex > H₄L > Ascorbic acid > Zn-complex > Cu-complex > Cd-complex > V-complex).

Keywords: Azo complexes, Azo dyes, Antioxidant effectiveness, Thermo gravimetric analysis, 2,4,6-Trihydroxyacetophenone.

Introduction

Azo dyes are a crucial component in the textile and printing industries; and they find applications in various fields, including food coloring, acid-base exponents, beam sensors, cosmetics, optical information retention, stimulated emission, LCD, and fiber-optical apparatus¹⁻³ Additionally, heteroaryl-based azo pigments have been found to have living utilization such as free radical inhibitor,

hygienic, antineoplastic, antidiabetic drug, and antiviral agents⁴⁻⁶. Azo-dyes contain a chromophore (-N=N-) which is a nitrogen-to-nitrogen double bond⁷⁻⁹. These dyes are produced by adding diazonium salt to a strongly activated aromatic system¹⁰⁻¹². The history of dyeing can be divided into two periods: the "pre-aniline" period, which lasted until 1856, and the "post-aniline" period. The former

was characterized by a limited range of colors that were produced from animals and plants¹³⁻¹⁵. Dyes are unsaturated and colored organic compounds that can dye a substrate, such as textiles. Disperse dyes are a type of water-insoluble dye that can dye acetate fibers, polyester, and other hydrophobic fibers like nylon, cellulose acetate, acrylic, polyester, and most manufactured fibers that lack ionizing groups¹⁶⁻¹⁸. Research was conducted on azo complexes that are used as antioxidants¹⁹⁻²¹. We did not find a study similar to our research. The research included preparing a new azo dye using as a ligand and then reacting it with some metal ions VO(II), Cu(II),

Zn(II), Cd(II) and Au(III) to create novel complexes of the mentioned metal ions²². In addition to characterization with spectroscopic analysis, thermal stability, and thermal decomposition were studied using DSC and TGA curves, and the antioxidant activity of these compounds was assessed against the DPPH radical and compared to that of a reference natural antioxidant, Ascorbic acid²³. This research aims to create novel complexes of the metal ions of VO(II), Cu(II), Zn(II), Cd(II), and Au(III) using the azo ligand H₂L. In addition to characterization the antioxidant activity of these compounds.

Materials and Methods

All the reactants, substances and firms for the prepared compounds were of analytical class. Absolute. Ethanol, dimethyl sulphoxide, and other solvents were of high purity and supplied by Merck Co., Fluka Co. and Sigma-Aldrich Co., and metal salts [3-aminophenol, 2,4,6-trihydroxyacetophenone, [NaNO₂, NaOH, ZnCl₂, CuCl₂.2H₂O, CdCl₂, HAuCl₄, VOSO₄.5H₂O] were supplied by Sigma-Aldrich Co. and BDH Co. The Bruker (400MHz) Spectrometer was used to obtain the ¹H & ¹³C NMR spectra. The melting point of the prepared compounds was measured by a Stuart electrothermal melting point apparatus. The elemental (C. H. N.) micro-analysis was used to search using the EA 3000 single V.3 model vector device. LC-MSQ-P-50-A(EI30ev) Shimadzu device. Infrared spectra were measured with a device (Shimadzu-8000S). Thermogravimetric curves (TG-DSC) were recorded using a device TGA Shimadzu. The ultraviolet-visible spectra of the ligand and its complexes were recorded using a Shimadzu UV-visible spectrophotometer. The balancing susceptibility model MSR-MKI utilized magnetic characteristics. Molar electrical conductivity measurements were carried out using BC3020 Professional Bench Top Conductivity device. Metals were determined using a Shimadzu (A-A) 680G atomic absorption spectrometer. The chlorine content was determined gravimetrically.

Synthesis of Ligand 1-(2,4,6-trihydroxy-3-((3-hydroxyphenyl)diazenyl)phenyl)ethan-1-one.

The synthesis process of the ligand is carried out in two steps, Scheme.1, first one is the preparation of diazonium salt at which (2g, 0.01mol) from 2,4,6-trihydroxyacetophenone dissolved in circular-bottomed flask its volume is 250 mL with the

mixture of (3 mL Hydrochloric acid HCl 37% with 35 ml distilled water DW) then the prepared mixture was cooled between 0-5 °C. After that the solution of (1g, 0.01mol.) sodium nitrate NaNO₂ that dissolved in 30 mL of distilled water was added to the last mixture as drop wise with continuous stirring, with good monitoring of temperature it must not rise more than 5 °C, for 30 minutes, the next step included the solution was left for 15 minutes resulting in diazonium salt as a product of the first step. Followed by diazotization coupling reaction between diazonium salt of 3-aminophenol and the solution of (3g, 0.03 mol.) (2,4,6-trihydroxyacetophenone) dissolved in 50 mL absolute Ethanol and 15 mL of 10% sodium hydroxide NaOH with cooling and continuous stirring during this process observed the precipitates were obtained in different colors. Fig. 1 shows both ¹H & ¹³C NMR data for the ligand. Proton NMR demonstrates the next chemical shifts a ppm: 2.6δppm (3H, Singlet), 7.5-8.0δppm (5H, multiplate), and 9.75-9.98δppm (4H, doublet). Corresponding to protons of methyl group of ketone, Ar-H protons and protons of phenolic groups respectively. On the other hand, carbon NMR spectrum which was tested using chloroform as solvent demonstrates the next peaks: 178.8 (C1), 137.4 (C2), 165 (C3), 156.2 (C4), 174.0 (C5), 155 (C6), 127.0 (C7), 182.0 (C8), 106.5 (C9), 190.0 (C10), 119.0 (C11), 170.0 (C12), 195.0 (C13), 49.9 (C14)²⁴⁻²⁶

Synthesis of Vanadium

To create the targeted complex, you need to add of (0.5g, 0.002mol) Azo ligand that has been dissolved in 15 ml absolute EtOH as a drop-wise addition, while continuously stirring. This should be added to the exact quantity of metal salt (0.30g, 0.002

mol)(VOSO₄.5H₂O) dissolved in 10 ml of distilled water. The mixture should then be heated and refluxed for six hours at 60°C. After this, let the mixture cool to room temperature and keep it in a cabinet for 24 hours to allow for complete formation and precipitation. Filter the solution and wash it with distilled water multiple times. Finally, wash it with a small quantity of hot EtOH. This product was collected after being filtered and dried. Its melting point was (231D) °C and dark red precipitate, and its yield was 77%.

Preparation of metallic metal ions complexes

Following the same approach used in Vanadyl complex synthesis, the complexes of the next

metalsalts.[CuCl₂.2H₂O](0.29g,0.002mol),(CdCl₂)(0.31g,0.002mol),(ZnCl₂)(0.24g,0.0017mol),(HAuCl₄)(0.68g,0.0014mol) were prepared. To dissolve the salts, 30 ml of ethanol and distilled water is used. Next, drop by drop we added the solution of salts to 30 ml of azo ligand weighting (0.5g,0.002mol). The mixture is then heated and refluxed for 6 hours at a temperature of up to 60°C. After that, any unreacted components are removed by briefly immersing them in hot ethanol. The solid complexes formed are then separated, collected, dried and weighted. The melting points of the complexes, colours and yields are listed in Table 1 below.

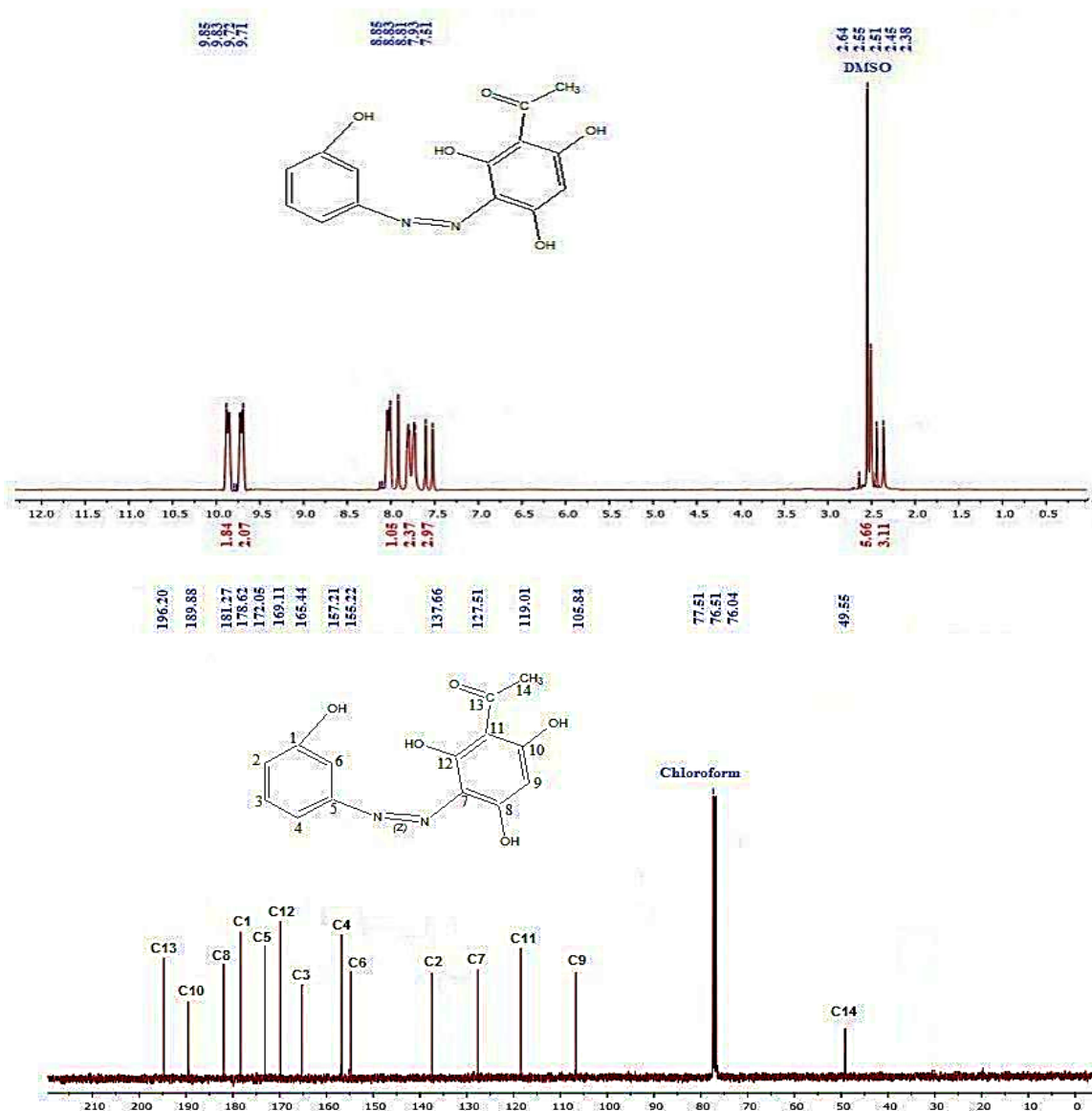
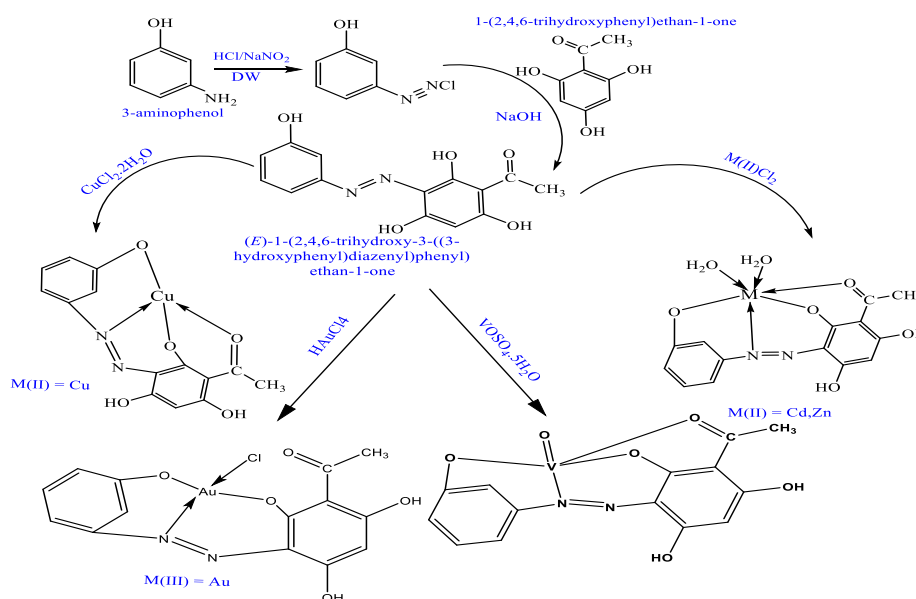


Figure 1. ¹H & ¹³C-(NMR) spectra of ligand



Scheme 1. Synthesis of ligand and its complexes.

Results and discussion

Table.1 shows the comparison between the estimated and theoretical results of the percentage of each element involved in synthesized complexes, as well as the chloride involvement and metal ratio. The

estimated results were obtained both technically and theoretically and were found to be in good agreement with each other.

Table 1. Micro elemental analysis, some physical features, metal ratio, and chloride content data

Compound (M. wt.)	Elemental microanalysis % found (calc.)					Yield%	M p°C	Color
	C	H	N	M	Cl			
C₁₄H₁₂N₂O₅ 288.26	57.89 (58.33)	4.67 (4.20)	10.11 (9.72)	--	--	50	146-148	Brown
C₁₄H₁₀N₂O₆V 353.18	47.99 (47.61)	3.46 (2.85)	8.88 (7.93)	13.91 (14.42)	--	77	231 D	Dark red
C₁₄H₁₀N₂O₅Cu 349.79	49.01 (48.07)	3.46 (2.88)	9.00 (8.01)	17.68 (18.17)	nil	61	264D	Brown
C₁₄H₁₄N₂O₇Zn 387.66	44.19 (43.38)	4.41 (3.64)	6.69 (7.23)	15.95 (16.87)	nil	85	184-186	Dark brown
C₁₄H₁₄N₂O₇Cd 434.68	39.33 (38.68)	3.98 (3.25)	7.34 (6.44)	26.81 (25.86)	nil	71	>300	Reddish brown
C₁₄H₁₀N₂O₅AuCl 518.66	33.19 (32.42)	1.14 (1.94)	6.19 (5.40)	37.25 (37.98)	7.10 (6.84)	76	193-195	Brown light

D=decompose

FT-IR Spectroscopy

Infrared spectroscopy determines the composition of new complexes by comparing the spectra of the complexes with the spectrum of the ligand. The modifications observed in the spectra of the complexes may involve changes in the intensities or shapes of the major bands, or a shifting in their wavelengths towards wave length low or high. In Fig. 2, the ligand exhibited the following extension a captivating and: A very strong band at 3580 cm⁻¹ belong to trembling of phenolic O-H, A strong to weak band at 3120 cm⁻¹ for the trembling of C-H

aromatic group, a weak band at 2912 cm⁻¹ belonging to C-H aliphatic group, a moderate, sharp band at 1631 cm⁻¹ for the vibrational mode of carbonyl group (C=O). Moreover, a unique band at 1463 cm⁻¹ was observed, which was not present in the starting materials, this band may be attributed to the vibrational mode of azo-group (N=N) and is considered strong evidence of azo formation²⁷. The cadmium complex shows the following absorption peaks: a weak stretching absorption band of the C-H aromatic group at 3000 cm⁻¹, overlapped with the broad band of the phenolic group (O-H) appearing at

3400 cm^{-1} . Additionally, we can clearly see the stretching weak band of the C-H aliphatic group at 2950 cm^{-1} . The change in the intensity of the azo-band that appeared at 1462 cm^{-1} may have happened due to the coordinative behavior with the metal ion through this group. The strong evidence that supports this fact is the appearance of a new band called M-N band at 524 cm^{-1} . The shifting in the location of the carbonyl absorption band compared to its location in the free ligand to be shown at 1612 cm^{-1} is also a good indication that proves the coordinative behavior through this group. Finally, the appearance of the Cd-O band at 443 cm^{-1} also proves the coordination through carbonyl and carbinol groups²⁸. The zinc complex exhibits various stretching absorption bands, including a broad band of phenolic group O-H, C-H aromatic group that overlaps with O-H and aqua group, C-H aliphatic group, azo-group (N=N), carbonyl group C=O, and carbinol group C-O. These bands were detected at 3473 cm^{-1} , 3178 cm^{-1} , 2926 cm^{-1} , 1462 cm^{-1} , 1598 cm^{-1} , and 1305 cm^{-1} , respectively. The same bands were observed in the ligand with some modifications, such as shifting and changing in their intensities due to the interaction with the metal ion. Additionally, there are new bands, including the aqua band H₂O (3415, 1620 and 657 cm^{-1}), Zn-N (524 cm^{-1}), and Zn-O (443 cm^{-1})²⁹, as displayed in Table 2. The Cupper complex exhibits several stretching absorption bands, including a broad band of phenolic group O-H, C-H aromatic group that overlaps with O-H, C-H aliphatic group, azo-group (N=N), carbonyl group C=O, and carbinol group C-O. These bands were detected at 3450 cm^{-1} , 3178 cm^{-1} , 2926 cm^{-1} , 1452 cm^{-1} , 1598 cm^{-1} , and 1307 cm^{-1} , respectively. These same bands

are observed in the ligand, but with some modifications such as shifting and changing in their intensities due to the interaction with metal ion. There are also new bands to consider, which are Cu-N and Cu-O at 520 cm^{-1} , 470 cm^{-1} respectively. Those bands are the same bands that observed in ligand with some modifications such as shifting and changing in their intensities due to the interaction with metal ion. The Au-complex exhibits several stretching absorption bands, including a broad band of phenolic group O-H, C-H aromatic group that overlaps with O-H, C-H aliphatic group, azo-group (N=N), carbonyl group C=O, and carbinol group C-O, these bands were detected at 3412 cm^{-1} , 3011 cm^{-1} , 2925 cm^{-1} , 1401, 1449 cm^{-1} , 1632 cm^{-1} , and 1305 cm^{-1} respectively. These same bands are observed in the ligand, but with some modifications such as shifting and changing in their intensities due to the interaction with metal ion. There are also new bands to consider, which are Au-N and Au-O at 510 cm^{-1} , 477 cm^{-1} respectively³⁰. Those bands are the same bands that observed in ligand with some modifications such as shifting and changing in their intensities due to the interaction with metal ion. for Vanadyl complex, displays the next stretching absorption bands: (broad band of phenolic group O-H, C-H aromatic group that overlapped with O-H and aqua groups, C-H aliphatic group, azo-groups (N=N), carbonyl group C=O and carbinol group C-O). Those bands were detected at (3406 cm^{-1} , 3100 cm^{-1} , 2900 cm^{-1} , 1401 cm^{-1} , 1625 cm^{-1} and 1136 cm^{-1}) respectively. Those bands are the same bands that observed in ligand with some modifications such as shifting and changing in their intensities due to the interaction with metal ion³¹.

Table 2. FT-IR spectral data for ligand and complexes

Compounds	(H ₂ O) aqua	(OH) phenolic	(C-H) aromatic	(C-H) aliphatic	(N=N)	C-O carbinol	(C=O)	M-N (M-O)
C ₁₄ H ₁₂ N ₂ O ₅ (H ₄ L)	--	3580	3120	2912	1463	1282	1631	--
C ₁₄ H ₁₀ N ₂ O ₅ Cd	3400 1620 657	3400	3000	2950	1456	1305	1612	524 (443)
C ₁₄ H ₁₂ N ₂ O ₆ ClZn	3415 1620 657	3473	3178	2926	1452	1305	1612	500 (466)
C ₁₄ H ₁₀ N ₂ O ₇ Cu	--	3450	3178	2926	1452	1307	1598	520 (470)
C ₁₄ H ₁₀ N ₂ O ₅ AuCl	--	3412	3011	2925	1449	1305	1632	510 (477)
C ₁₄ H ₁₀ N ₂ O ₆ V	--	3406	3100	2900	1401	1136	1625	493 (478)

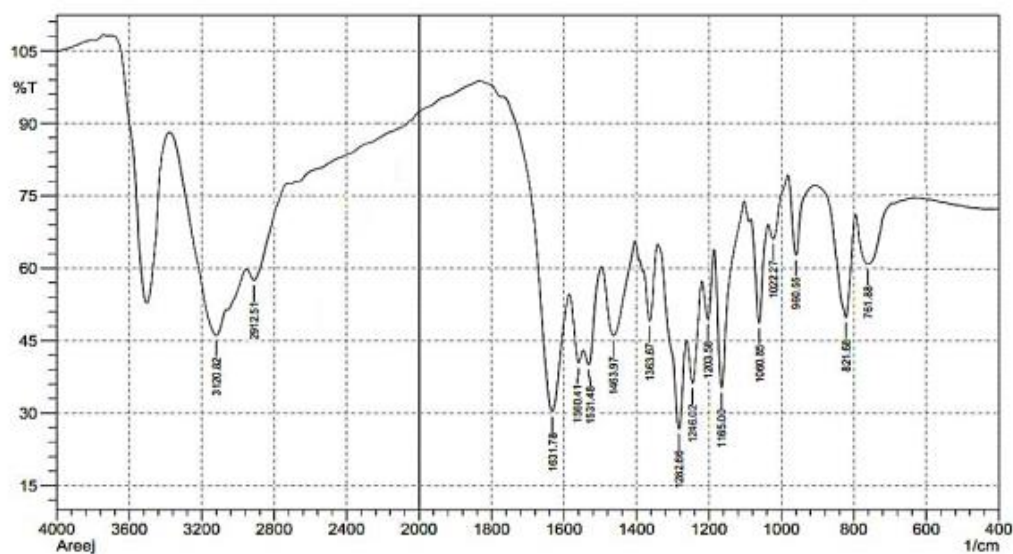


Figure 2. FT-IR spectrum for ligand

Electronic spectra for compounds molar conductivity and magnetic susceptibility

The UV-vis spectrum of ligand which Fig. 3 shows with a moderately broad absorption band at 300 nm, 33333 cm^{-1} corresponding to ($\pi \rightarrow \pi^*$) electronic transition, and another broad band at 391 nm, 25575 cm^{-1} corresponding to $n \rightarrow \pi^*$ electronic transition³². Fig. 4 demonstrates the spectrum of Copper complex and the next transitions: ($\pi \rightarrow \pi^*$, $n \rightarrow \pi^*$ and C. T M \rightarrow L) at (245 nm, 40816 cm^{-1}), (265 nm, 37735 cm^{-1}) respectively. The transitions of ligand with some shifting in their wavelengths because of coordination with metal. In addition to d-d transitions at visible region (570 nm, 17543 cm^{-1}) belonging ${}^2T \rightarrow {}^2E$. $\mu_{\text{eff}} = 1.76$ which is an indicative of a Tetrahedral geometry³³. The spectrum of Cadmium complex and the next transitions: ($\pi \rightarrow \pi^*$, $n \rightarrow \pi^*$ and C. T M \rightarrow L) at (295 nm, 33898 cm^{-1}), (350 nm, 28571 cm^{-1}) and (395 nm, 25316 cm^{-1}) respectively the transitions of ligand with some shifting in their wavelengths because of coordination with metal. The spectrum of Zinc complex and the next transitions: ($\pi \rightarrow \pi^*$, $n \rightarrow \pi^*$ and C. T M \rightarrow L) at (371 nm, 26932 cm^{-1}), and (509 nm, 19623 cm^{-1}) respectively the transitions of ligand with some shifting in their wavelengths because of coordination with metal. The complexes of zinc and cadmium is diamagnetic and their μ_{eff} is equal to zero which is indicative of an Octahedral geometry. The UV-Vis spectrum of Au-complex demonstrates the next electronic transition peaks: ($\pi \rightarrow \pi^*$) at (306 nm, 33679 cm^{-1}) and intra ligand at (387 nm, 25839 cm^{-1}). The previous transitions resemble to those found in the ligand itself and the noticeable shifting proves the occurrence of coordination with metal. Other electronic transitions

attribute to the transitions in metal itself (d-d) transitions, those are as follows: ${}^1A_{1g} \rightarrow {}^1B_{1g}$ and ${}^1A_{1g} \rightarrow {}^1E_g$ observed at (667 nm, 14992 cm^{-1}) and (739 nm, 13531 cm^{-1}) respectively which support the square planer geometry³⁴. The UV-Vis spectrum of vanadium complex displays the next transitions: at ultra-violet region ($\pi \rightarrow \pi^*$ and $n \rightarrow \pi^*$) transitions corresponding to (280 nm, 35714 cm^{-1} and 310 nm, 32258 cm^{-1}) respectively. Additionally, to transitions of d-d at visible region at (490 nm, 20408 cm^{-1}) and (630 nm, 15873 cm^{-1}) had attributed to ${}^2B_2 \rightarrow {}^2B_2$ and ${}^2B_2 \rightarrow {}^2B_1$ transitions³⁵. The electronic spectrum of the Au(III) compound was studied, exhibits peak of (362, 489 and 568) nm assigned to $\pi \rightarrow \pi^*$, ${}^1A_{1g} \rightarrow {}^1B_{1g}$ and ${}^1A_{1g} \rightarrow {}^1A_{2g}$ respectively which is an indicative of a square planer geometry. All complexes exhibit the same absorption bands as those found in the ligand, located in the ultraviolet region. However, there are some alterations, involving a shifting in absorption bands due to the coordination binding with metal ions. Furthermore, a new absorption peaks were show in the visible region, which belong to transitions of d-d, as shown in Table 3. The molar conductivity of the synthesized complex solutions was measured by preparing $1 \times 10^{-3}\text{ M}$ from the complexes in DMSO solvent at room temperature. It was found that all measurements shown in Table 3 were consistent with the suggested structural formula of all complexes, indicating that all complexes are non-electrolytes and confirming the geometries of the obtained complexes. Magnetic susceptibility measurements have been widely used in the diagnosis and study of complex transition metals. The most important aspect in this field relates to the effects resulting from the partially filled outer

casings with electrons. Magnetic measurements provide information about the compound in terms of the electronic arrangement and the oxidation state of the transition metal atoms. The number of lone electrons of a transition metal ion indicates the state of the spin of the studied complex, whether it is spinning low or high³⁶.

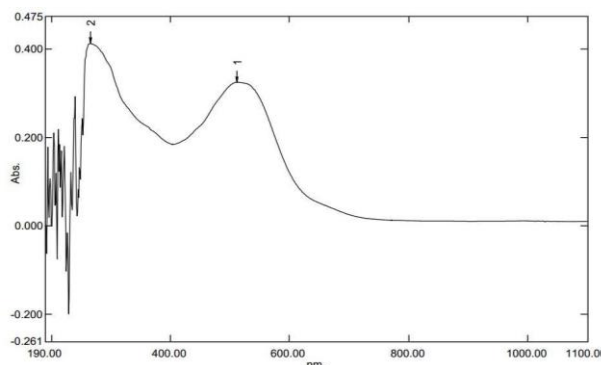
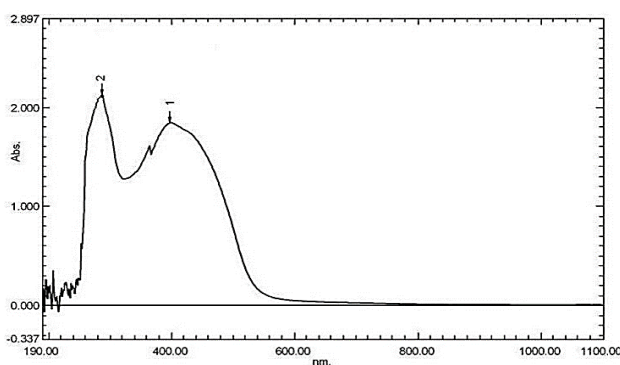


Figure 3. UV-vis spectrum of Ligand Figure 4. UV-Vis spectrum of Cu-complex

Table 3. Electronic spectral data of the compounds and magnetic moment

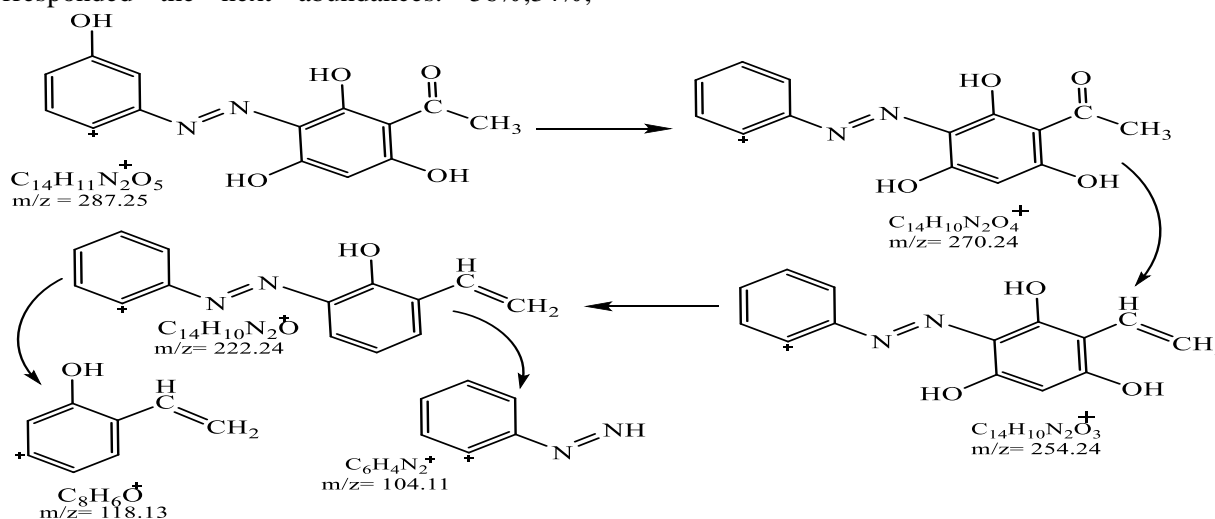
Compound	λ_{max} (nm)	$\nu_{cm^{-1}}$	ABS.	$\epsilon_{max} L mol^{-1} cm^{-1}$	$\Lambda_m cm^2 \Omega^{-1} mol^{-1}$	Assignment	μ_{eff}
$C_{14}H_{12}N_2O_5$ (H ₄ L)	300	33333	2.090	2090	--	$\pi \rightarrow \pi^*$	-
	391	25575	1.850	1850		$n \rightarrow \pi^*$	
$C_{14}H_{12}N_2O_6ClCu$ Tetrahedral	245	40816	0.300	300.0	15	$\pi \rightarrow \pi^*$	1.76
	265	37735	0.410	410.0		$n \rightarrow \pi^*$	
	570	17543	0.400	400.0		C.T (M→L) $^2T \rightarrow ^2E$	
$C_{14}H_{12}N_2O_6ClCd$ Octahedral	295	33898	2.200	220	19	$\pi \rightarrow \pi^*$	Diamagnetic
	350	28571	0.050	50.0		$n \rightarrow \pi^*$	
	390	25641	0.800	800		$n \rightarrow \pi^* + C.T$ (M→L)	
$C_{14}H_{10}N_2O_5Zn$ Octahedral	371.3	26932	0.521	521	11	$\pi \rightarrow \pi^*$	Diamagnetic
	509.6	19623	0.120	120		C.T (M→L)	
$C_{14}H_{10}N_2O_5AuCl$ Square Planar	362	27624.3	4.0	4000	17	$\pi \rightarrow \pi^*$	Diamagnetic
	489	20449.8	1.18	1180		$n \rightarrow \pi^*$	
	568	17605.6	1.70	1700		$^1A_{1g} \rightarrow ^1B_{1g}$ $^1A_{1g} \rightarrow ^1E_g$	
$C_{14}H_{10}N_2O_6V$ (Trigonal Bipyramid)	280	35714	0.400	400	9	$\pi \rightarrow \pi^*$	1.77
	310	32258	0.550	550		$n \rightarrow \pi^*$	
	450	22222	0.680	680		C.T M→L	
	490	20408	0.500	500		$^2B_2 \rightarrow ^2B$	
	630	15873	0.600	600		$^2B_2 \rightarrow ^2B_1$	

LC-Mass spectra for ligand and some complexes: LC-Mass spectrum testing is one of the most crucial methods for characterizing the ligand and some products. It supplements other methods that estimate the molecular weight of the chemical. The fragmentation pattern and the extract mass for each pattern are shown in Scheme 2 to provide mass information for the ligand. The fragment's molecular ion peak $[M]^+$ is easily visible, such as $C_{14}H_{11}N_2O_5^+$

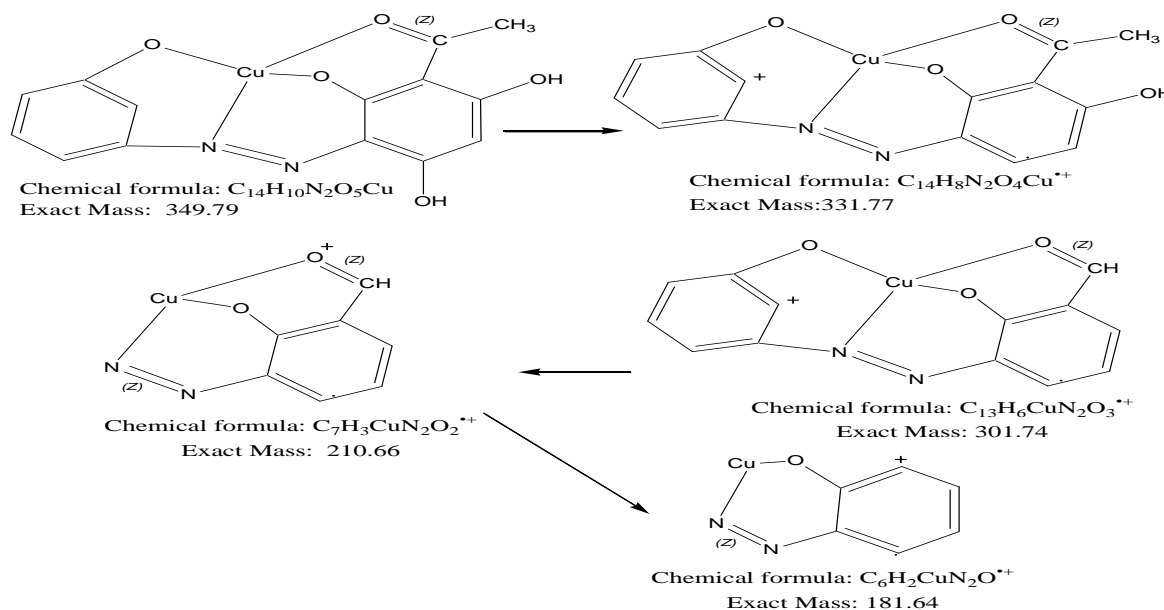
with a relative abundance of about 9% in Fig. 5. Other abundances are also present for the rest of the peaks: $C_{14}H_{10}N_2O_4^+$, $C_{14}H_{10}N_2O_3^+$, $C_{14}H_{10}N_2O^+$, $C_8H_6O^+$ and $C_6H_4N_2^+$ corresponded the next abundances: 270.24 m/z, 254.24 m/z, 222.24 m/z, 118.13 m/z and 104.11 m/z respectively³⁷. For copper complex, Fig.6 and Scheme 3, we can also detect the molecular ion peak (M^+) at 349.79 m/z with relative abundance 16% and next

pattern: $C_{14}H_8N_2O_4Cu^+$, $C_{13}H_6CuN_2O_3^{+}$, $C_7H_3CuN_2O_2^+$, $C_6H_2CuN_2O^+$ corresponded to: 331.97 m/z, 301.74 m/z, 210.66 m/z, 181.64 m/z respectively, corresponded the next abundances: 44%, 49%, 48%, 60% respectively. For Au-complex, Scheme 4, we can also detect the molecular ion peak (M^+) at 518.66 m/z with relative abundance 20% and next pattern: $C_{14}H_9AuClN_2O_4^+$, $C_{12}H_6AuClN_2O_3^+$, $C_{12}H_6AuN_2O_3^+$, $C_6H_3AuNO^+$, $C_6H_3NO_2^+$ corresponded to: 501.65 m/z, 458.61 m/z, 423.15 m/z, 302.06 m/z, 121.09 m/z respectively, For Zinc complex, Scheme 5, we can also detect the molecular ion peak (M^+) at 387.66 m/z with relative abundance 24% and next pattern: $C_{14}H_{11}N_2O_6Zn^+$, $C_{14}H_8N_2O_4Zn^+$, $C_6H_3N_2O_4Zn^+$, $C_8H_6O_3^+$ corresponded to: 368.64 m/z, 333.61 m/z, 184.49 m/z, 302.06 m/z, 150.13 m/z respectively corresponded the next abundances: 56%, 34%,

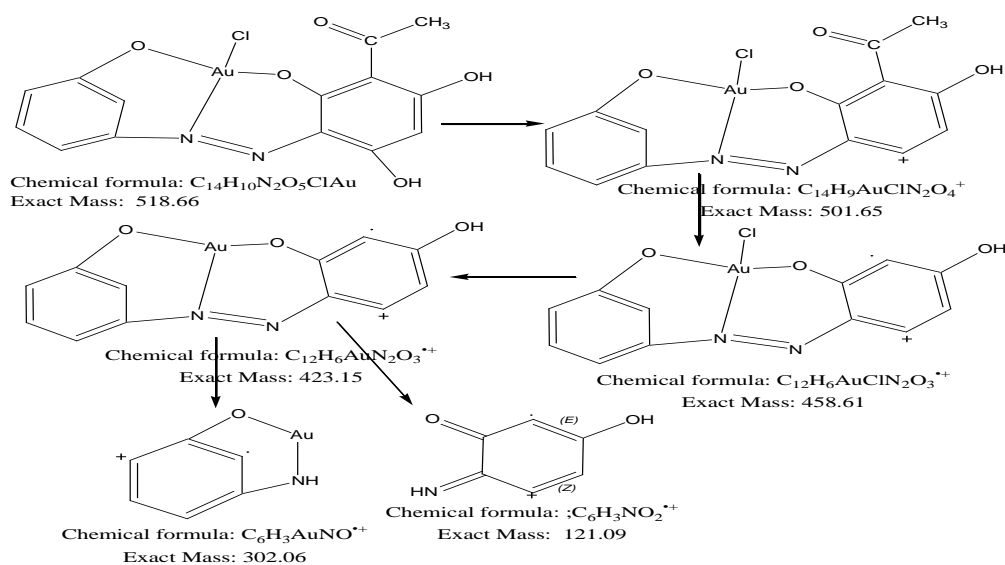
63%, 72% respectively. For Cadmium complex, Scheme 6, we can also detect the molecular ion peak (M^+) at 434.68 m/z with relative abundance 10% and next pattern: $C_{14}H_{11}N_2O_6Cd^+$, $C_{14}H_8N_2O_4Cd^+$, $C_{13}H_6CdN_2O_4^+$, $C_7H_3CdN_2O_3^+$, $C_6H_2CdN_2O_2^+$ corresponded to: 415.66 m/z, 380.64 m/z, 366.61 m/z, 275.52 m/z, 246.50 m/z respectively corresponded the next abundances: 22%, 48%, 36%, 34%, 28% respectively. For vanadium complex show the molecular ion peak (M^+) for $C_{14}H_{10}VN_2O_6$ formula at 353 m/z which matches the molecular weight of the complex³⁸. Moreover, the next fragmentation patterns were also observed in the spectrum: ($C_{14}H_{10}VN_2O_4$ m/z = 321.18, $C_{12}H_8VN_2O_3$ m/z = 279.15, $C_{12}H_8VN_2O_2$ m/z = 263.15, $C_6H_4NO_2$ m/z = 123.11 and C_6H_4NV m/z = 141.04)³⁹.



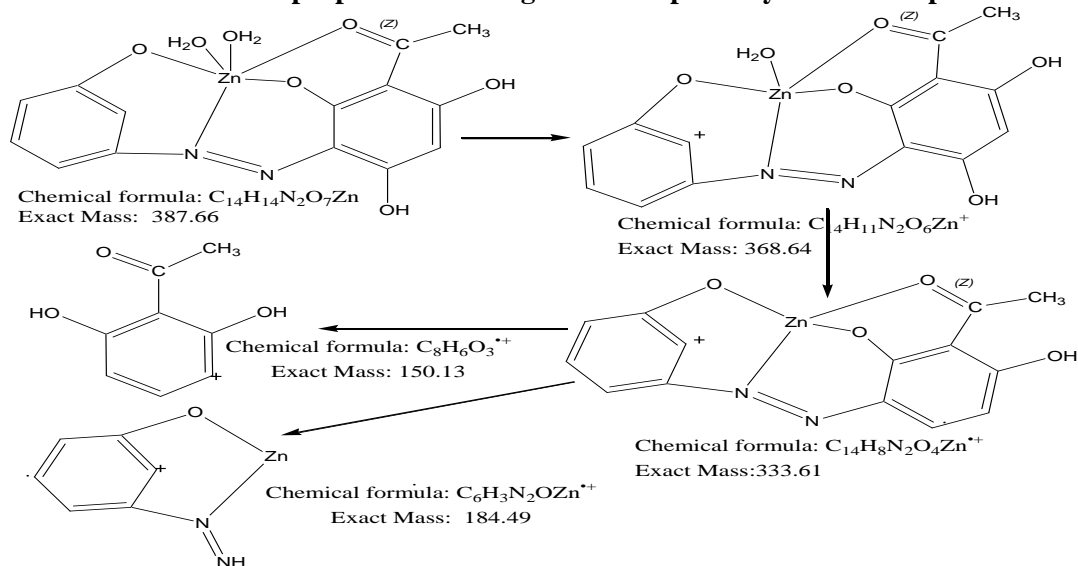
Scheme 2. The proposed mass fragmentation pathways of ligand



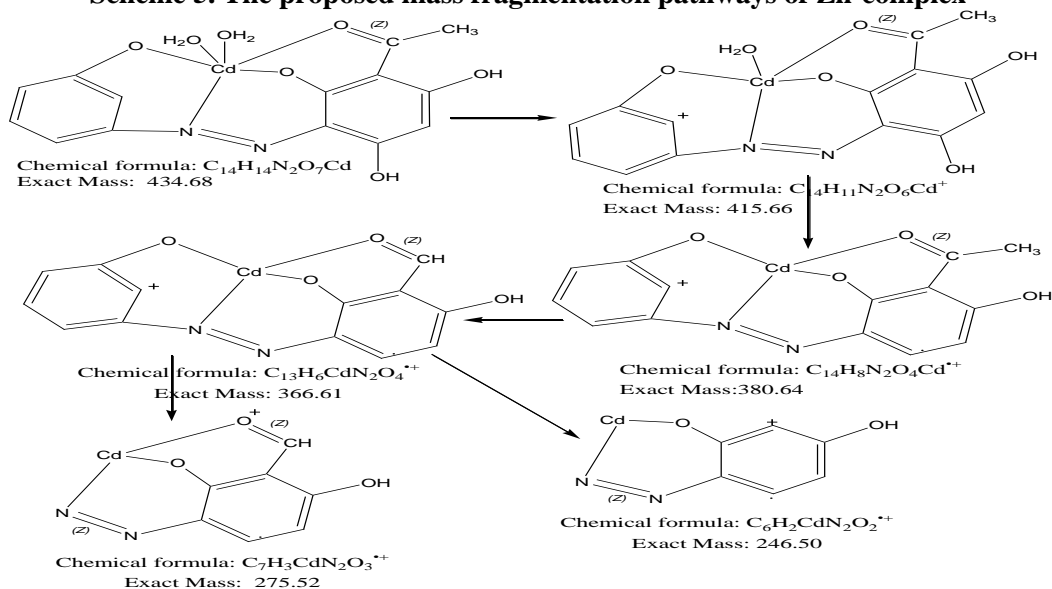
Scheme 3. The proposed mass fragmentation pathways of Cu-complex



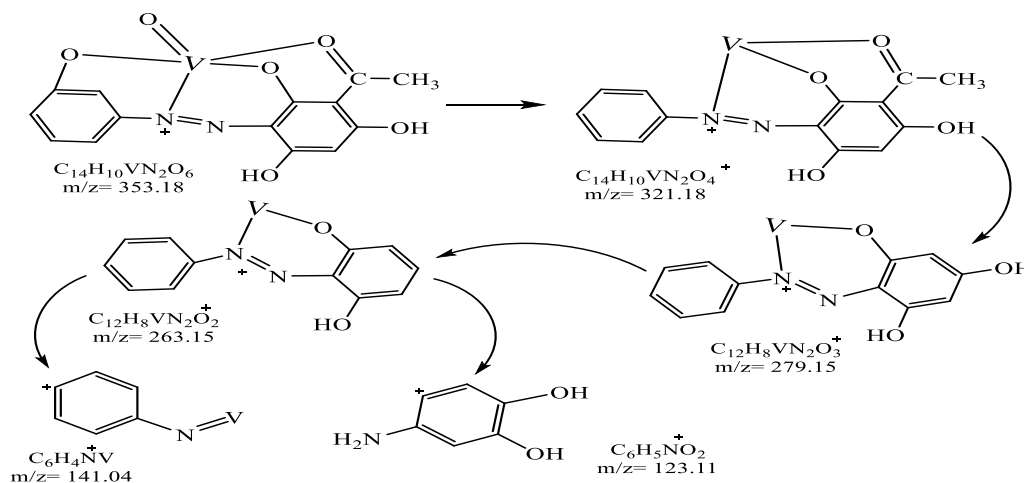
Scheme 4. The proposed mass fragmentation pathways of Au-complex



Scheme 5. The proposed mass fragmentation pathways of Zn-complex



Scheme 6. Partitioning analogues for Cd-complex



Scheme 7. Partitioning analogues for Vanadium complex

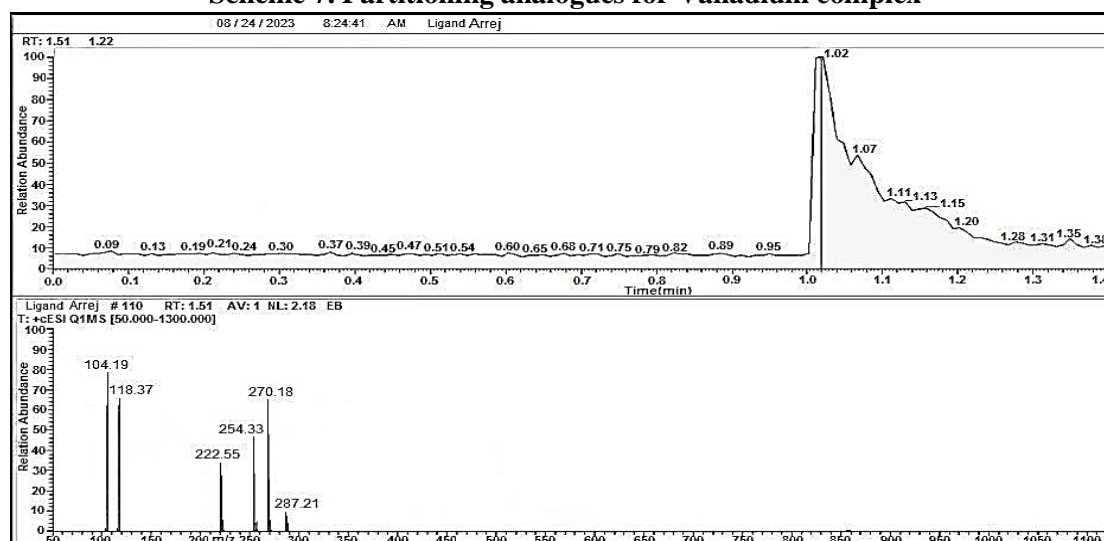


Figure 5. LC-Mass spectrum of ligand (H₄L)

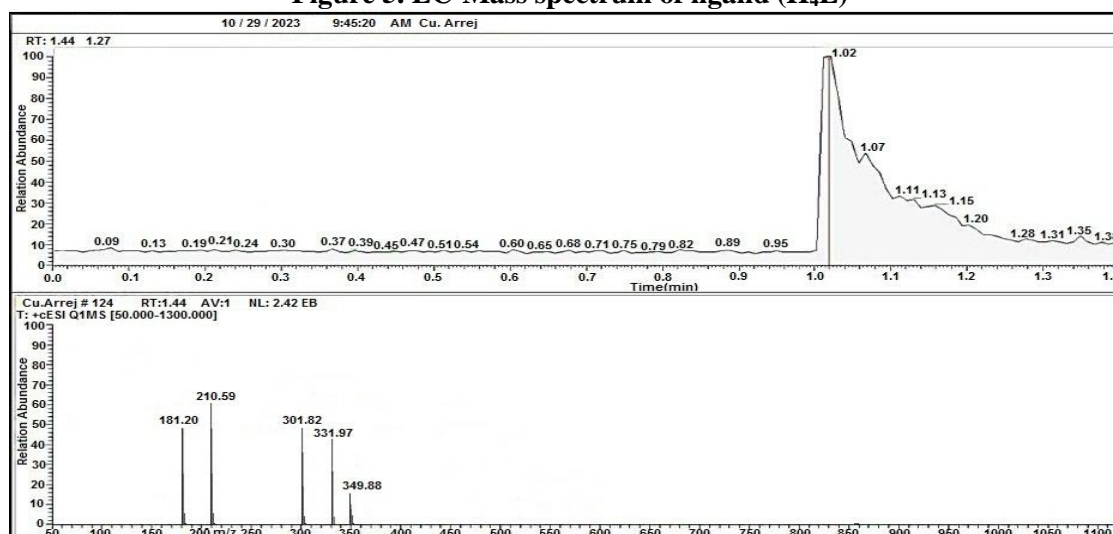


Figure 6. LC-Mass spectrum of Cu-complex

Thermal Analysis Diagnosis

DSC (differential scanning calorimetry) is a pyrolysis technique that helps to determine the amount of temperature absorbed and released during

thermal changes in a substance. It is widely used in various fields such as minerals, organic compounds, pharmaceuticals, polymers, inorganic substances and food to determine their purity and stability. Ti/°C,

Tf/°C and heat amount ΔH J/g enthalpy in units are measured for exothermic or endothermic reactions, ΔS entropy a measure of the unavailable energy in a closed thermodynamic system that is also usually considered to be a measure of the system's disorder, that is a property of the system's state, and that varies directly with any reversible change in heat in the system and inversely with the temperature of the system all compounds undergo regular thermal decomposition in their final stages, and ΔG energy Gibbs the standard Gibbs free energy change, ΔG°, indicates the thermodynamic favorability of a physical or chemical process. When ΔG° < 0, the process is thermodynamically favored. For a given process, the value of ΔG° can be calculated directly from the values of ΔH° and ΔS° using the following equation: ΔG° = ΔH° - TΔS°, all processing is

thermodynamically favored, as shown in Table 4 Figs. 7,8. Thermal study of ligand and some complexes are done using TGA (thermogravimetric analysis) and DSC curves. TGA measures the mass change of a substance with temperature when subjected to a controlled thermal program in a specific time. The obtained curve is referred to as a thermogravimetric curve and gives information about thermal stability, reaction rates, chemical structure, and the thermal stability of the products. The thermal behavior of ligand and Zn-complex was characterized using thermogravimetric analysis curve (TGA) Figs.9-10. Schemes 7-8 give identical results with suggested chemical formula of ligand and tested complex and also demonstrate information for each pyrolysis step that occurred³⁸⁻⁴⁰.

Table 4. Differential scanning calorimetry data for ligand and some complexes

Compound	T _i /°C	T _f /°C	Max. T. point °C	ΔH J/g	ΔS J	ΔG J	Type
C ₁₄ H ₁₂ N ₂ O ₅	387.65	395.13	7.48	-3.43	-0.4588	-183.463	endothermic
C ₁₄ H ₁₀ N ₂ O ₅ Zn	70.38	121.40	51.02	-103.51	-1.039	-0.00482	Endothermic
	127.10	188.48	61.38	-222.65	-1.410	-0.152	Endothermic
	216.97	277.592	60.62	-16.22	-0.075	32.35	Exothermic
	230.45	67.67	37.22	-88.47	-0.352	-0.12256	Endothermic
C ₁₄ H ₁₀ N ₂ O ₆ V	111.25	595.955	484.705	-39.70	-0.154	79.388	Exothermic

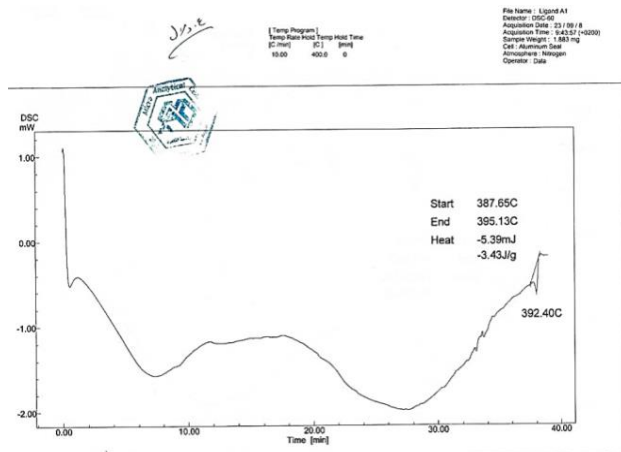


Figure 7. DSC. Curve for ligand Figure 8. DSC. Curve for Zn complex

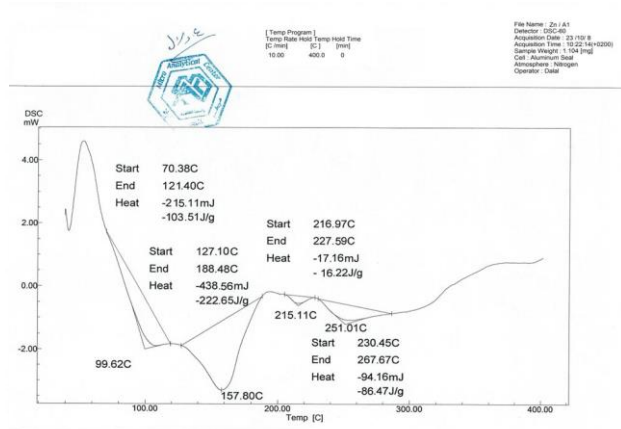
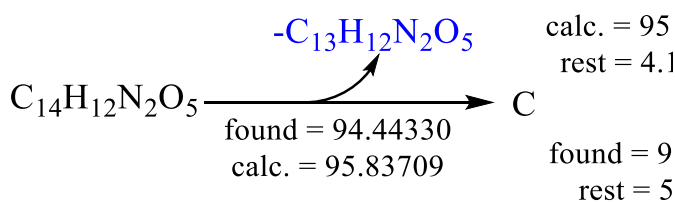
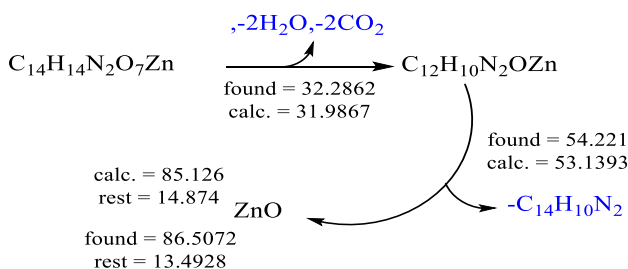


Table 5. Thermo gravimetric analysis data for ligand and some complexes

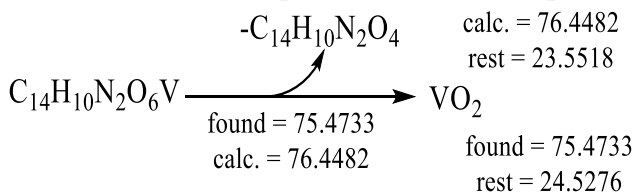
Compound (M. wt.)	% Estimated (calculated)		Assignment
	Mass loss	Total mass loss	
C ₁₄ H ₁₂ N ₂ O ₅ 288.26	94.4433 (95.837)	94.4433 (95.837)	-C ₁₃ H ₁₂ N ₂ O ₅ C
Calculated: 95.837% final = 4.16291%; Estimated 94.4433 % final = 5.5567%			
C ₁₄ H ₁₀ N ₂ O ₆ V 345.17	(76.4482) 75.4733	(76.4482) 75.4733	-C ₁₄ H ₁₀ N ₂ O ₄
Calculated: 76.4482% final = 23.5518%; Estimated 75.4733% final = 24.5276%			
C ₁₄ H ₁₂ N ₂ O ₇ Zn 387.66	32.2862(31.9867)	54.221(53.1393)	-2H ₂ O, -2CO ₂ -C ₁₄ H ₁₀ N ₂
Calculated: 85.126% final = 14.874%; Estimated 86.5072% final = 13.4928%			



Scheme 8. Pyrolysis pathway for ligand



Scheme 9. Pyrolysis pathway for Zn-Complex



Scheme 10. Pyrolysis pathway for vanadyl complex

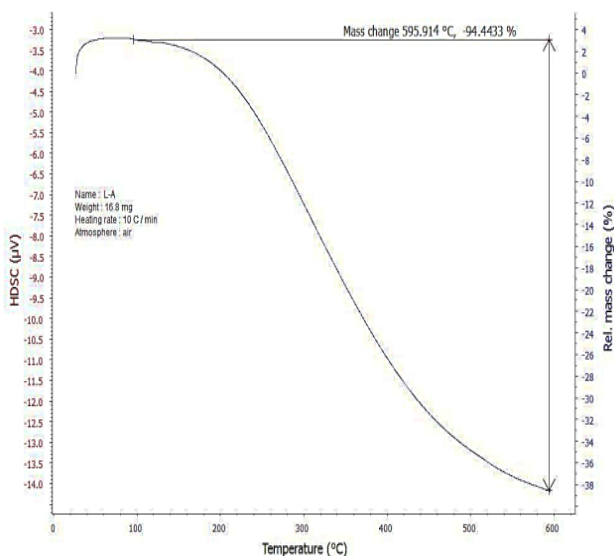


Figure 9. Thermo gravimetric analysis of ligand

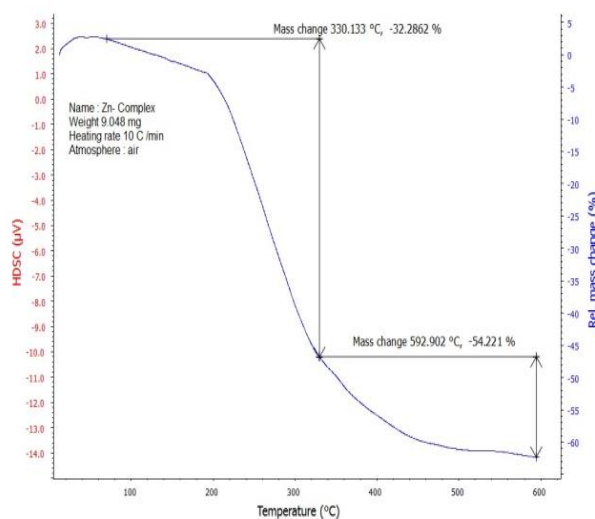


Figure 10. Thermo gravimetric analysis of Zn complex

Determination of DPPH radical scavenging efficiency

The inhibitory effect of ligand and its minerals, including Cu(II), Zn(II), Cd(II), VO(II) and Au(III) on reactive oxygen species was evaluated using DPPH. The combination of the ligand and its mineral causes a change in color of DPPH from purple to yellow due to the transfer of hydrogen from the ligand to the DPPH molecule. The color conversion was detected using a UV-Vis spectrophotometer at 517 nm. The Radical scavenging activities of the ligand and its minerals on reactive oxygen species was ranked in the following order: Au-complex > H₄L > Ascorbic acid > Zn-complex > Cu-complex > Cd-complex > V-complex based on the higher IC₅₀ value indicating lower antioxidant effectiveness³²⁻³⁴. The ligand and molybdenum complex demonstrated higher antioxidant activity³⁵⁻³⁷. The free radical scavenging effects of all the compounds with the DPPH radical were evaluated using the following Eq.1 and presented in Table 5 under the same conditions³⁸⁻⁴⁰.

$$\text{PI \%} = \frac{\text{Absorbance of control} - \text{Absorbance of sample}}{\text{Absorbance of control}} \times 100\% \quad \dots\dots 1$$

PI = Percentage Inhibition

RSA = 100 - PI; : RSA = Radical Scavenging Activity

Table 5. Radical scavenging activities, Percentage Inhibition and IC₅₀ values

Compound	Conc. µg/ml	PI %	RSA %	IC ₅₀
C₁₄H₁₂N₂O₅	0.375	9.95	90.05	0.019
	0.186	42.17	57.83	
	0.093	58.99	41.01	
	0.046	66.08	33.92	
Cu-Complex	0.068	10.13	89.87	0.027
	0.034	35.18	64.82	
	0.017	50.25	49.75	
	0.008	57.92	42.08	
Zn-Complex	0.076	21.05	78.95	0.025
	0.038	38.43	61.57	
	0.019	45.48	54.52	
	0.009	53.12	46.88	
Cd-Complex	0.084	20.46	79.54	0.029
	0.042	38.43	61.57	
	0.021	46.03	53.97	
	0.010	54.18	45.82	
Au-Complex	0.049	22.46	77.54	0.018
	0.024	48.03	51.97	
	0.012	51.33	48.67	
	0.006	56.78	43.22	
V-Complex	0.664	59.48	40.52	0.199
	0.332	74.38	25.62	
	0.166	79.49	20.51	
	0.083	84.38	15.62	
Ascorbic acid	0.374	12.29	87.80	0.023
	0.186	36.75	63.25	
	0.03	58.74	41.26	

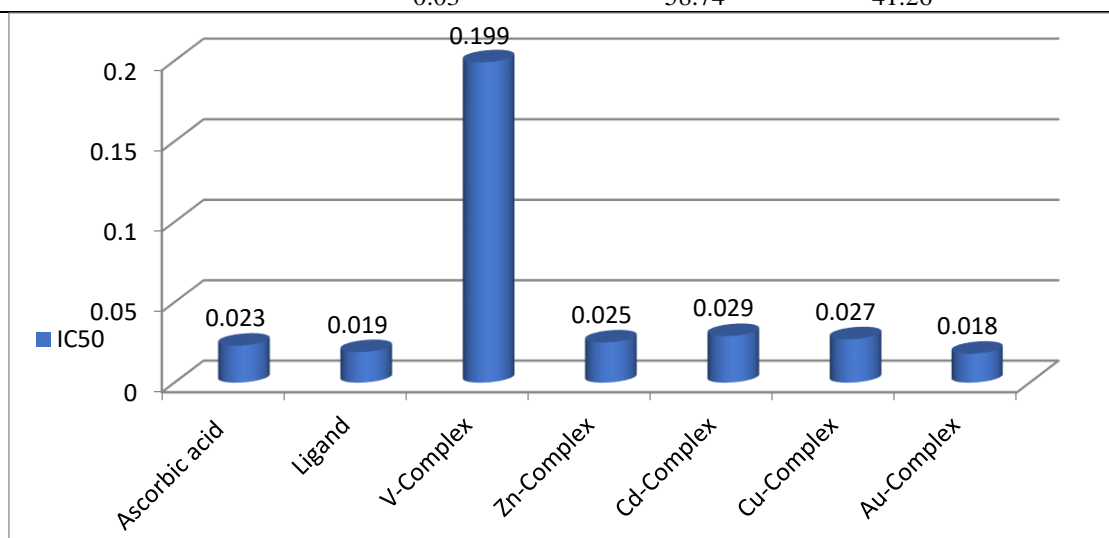


Figure 11. Variations of IC₅₀ values for ligand and its complexes

Conclusion

The Azo-dye ligand, known as H₄L, was synthesized through the diazotization process. This involved the reaction of the diazonium salt of 3-aminophenol with 2, 4, 6-trihydroxy acetophenone. The resulting product was the ligand (E)-1-(2,4,6-trihydroxy-3-((3-hydroxyphenyl) diaziny)phenyl)ethan-1-one =

(H₄L). Stable azo-ligand complexes were successfully synthesized by reacting the azo-ligand with various metal ions, including Cu(II), Cd(II), Zn (II), VO(II) and Au (III). This binding of metal ions occurred through the oxygen and nitrogen atoms of the azo-group in the ligand. The formation of M-O

and M-N bands, which do not occur in the spectrum of free ligand, clearly indicated the interaction of metal ions with the ligand. FT-IR study of the compounds revealed the shifting of carbinol and carbonyl absorption bands, which are attributed to the coordination through these groups. Furthermore, the spectra indicated the binding of aqua water molecules in some complexes. Based on electronic spectra and molar conductivity measurements, we were able to confirm that all complexes had octahedral shapes, except for the Copper complex, which had a tetrahedral shape and Au-complex which had square planar shape. LC-Mass spectra, the fragmentation cognate of the complexes, and elementary diagnoses establish the molecular formulas obtained through comparing the theoretical

and experimental results. Thermal identification tests showed whether water molecules were included in some complexes or excluded, and this test also demonstrated the various stabilities of the compounds. Finally, the antioxidant effectiveness of the compounds was tested using DPPH and ascorbic acid as a standard, with satisfactory results. The Radical scavenging activities of the ligand and its minerals were ranked in order of inhibitory activity on reactive oxygen species as follows: Au-complex > H₄L > Ascorbic acid > Zn-complex > Cu-complex > Cd-complex > V-complex. This ranking included the higher antioxidant activity of the synthesized azo-dye due to the presence of four hydroxyl-groups, as detailed in the manuscript.

Acknowledgment

Authors would like to thank everyone that contributed to the success of this review article, we extend our thanks to the Department of Chemistry, College of Science for women, Baghdad University,

Ministry of Higher Education & Scientific Research & Science and Technology, Directorate of Environment & Water.

Authors' Declaration

- Conflicts of Interest: None.
- We hereby confirm that all the Figures and Tables in the manuscript are ours. Furthermore, any Figures and images, that are not ours, have been included with the necessary permission for re-publication, which is attached to the manuscript.

- Ethical Clearance: The project was approved by the local ethical committee at Ministry of Education.
- No animal studies are present in the manuscript.
- No human studies are present in the manuscript.
- No potentially identified images or data are present in the manuscript.

Author's Contributions Statement

This work carried out in collaboration between all authors. A. M. F. prepared the samples, wrote and edited the manuscript with revision. A. A. S. did the

tests and interpreted the data with revision. and W. Al.Z. did the tests of antioxidants and listed their data in the manuscript.

References

1. Hamza IS, Mahmmoud WA, Al-Hamdani AA, Ahmed SD, Allaf AW, Al Zoubi W. Synthesis, characterization, and bioactivity of several metal complexes of (4-Amino-N-(5-methyl-isaxazol-3-yl)-benzenesulfonamide). *Inorg Chem Commun.* 2022; 144: 109776. <https://doi.org/10.1016/j.inoche.2022.109776>
2. Mahmudov KT, Gurbanov AV, Aliyeva VA, Resnati G, Pombeiro AJ. Pnictogen bonding in coordination chemistry. *Coord Chem Rev.* 2020 Sep 1; 418: 213381. <https://doi.org/10.1016/j.ccr.2020.213381>
3. El-Gammal OA, Mohamed FS, Rezk GN, El-Bindary AA. Synthesis, characterization, catalytic, DNA binding and antibacterial activities of Co (II), Ni (II) and Cu (II) complexes with new Schiff base ligand. *J Mol Liq.* 2021; 15(326): 115223. <https://doi.org/10.1016/j.molliq.2020.115223>
4. Jain S, Dongare K, Nallamothe B, Dora CP, Kushwah V, Katiyar SS. Enhanced stability and oral bioavailability of erlotinib by solid self nano emulsifying drug delivery systems. *Int J Pharm.* 2022; 622: 121852. <https://doi.org/10.1016/j.ijpharm.2022.121852>
5. Khedr AM, El-Ghamry H, Kassem MA, Saad FA, El-Guesmi N. Novel series of nanosized mono-and homobinuclear metal complexes of sulfathiazole azo

- dye ligand: Synthesis, characterization, DNA-binding affinity, and anticancer activity. *Inorg Chem Commun.* 2019; 1(108): 107496. <https://doi.org/10.1016/j.inoche.2019.107496>
- Al-Hassani RA. Synthesis, Characterization, Antimicrobial and Theoretical Studies of V (IV), Fe (III), Co (II), Ni (II), Cu (II), and Zn (II) Complexes with Bidentate (NN) Donor Azo Dye Ligand. *Baghdad Science Journal.* 2016 Dec 4;13(4):0793-. <https://doi.org/10.21123/bsj.2016.13.4.0793>.
 - Mallikarjuna NM, Keshavayya J. Synthesis, spectroscopic characterization and pharmacological studies on novel sulfamethaxazole based azo dyes. *J King Saud Univ Sci.* 2020; 32(1): 251-9. <https://doi.org/10.1016/j.saa.2013.09.070>
 - Abdallah SM, Zayed MA, Mohamed GG. Synthesis and spectroscopic characterization of new tetradentate Schiff base and its coordination compounds of NOON donor atoms and their antibacterial and antifungal activity. *Arab J Chem.* 2010; 3(2): 103-13. <https://doi.org/10.1016/j.arabjc.2010.02.006>
 - Kumar DN, Garg BS. Synthesis and spectroscopic studies of complexes of zinc (II) with N₂O₂ donor groups. *Spectrochim Acta- A: Mol Biomol Spectrosc.* 2006; 64(1): 141-147. <https://doi.org/10.1016/j.saa.2005.07.008>
 - Sahar YJ, Mohammed HS. Synthesis and characterization some complexes of azo dye of pyrimidynyl and evaluating their biological activity. *QJPS.* 2019; 24(3): 179-201.
 - Deghadi RG, Mahmoud WH, Mohamed GG. Metal complexes of tetradentate azo-dye ligand derived from 4, 4-oxydianiline: Preparation, structural investigation, biological evaluation and MOE studies. *Appl Organomet Chem.* 2020; 34(10): e5883. <https://doi.org/10.1002/aoc.5883>
 - Al Zoubi W, Ko YG. Self-assembly of hierarchical N-heterocycles-inorganic materials into three-dimensional structure for superior corrosion protection. *J Chem. Eng.* 2019; 356: 8506. <https://doi.org/10.1016/j.ccej.2018.09.089>
 - Mohammed H. Synthesis, identification, and biological study for some complexes of azo dye having theophylline. *Sci World J.* 2021 Jul 22; 2021. <https://doi.org/10.1155/2021/9943763>
 - Waheeb AS, Kyhoiesh HA, Salman AW, Al-Adilee KJ, Kadhim MM. Metal complexes of a new azo ligand 2-[2'-(5-nitrothiazolyl) azo]-4-methoxyphenol (NTAMP): Synthesis, spectral characterization, and theoretical calculation. *Inorg. Chem. Commun.* 2022;138:109267. <https://doi.org/10.1016/j.inoche.2022.109267>
 - Mahmudov KT, Gurbanov AV, Aliyeva VA, Resnati G, Pombeiro AJ. Pnictogen bonding in coordination chemistry. *Coord Chem Rev.* 2020; 1; 418: 213381. <https://doi.org/10.1016/j.ccr.2020.213381>
 - Al-Khateeb ZT, Karam FF, Al-Adilee K. Synthesis and characterization of some metals complexes with new heterocyclic azo dye ligand 2-[2--(5-Nitro thiazolyl) azo]-4-methyl-5-nitro phenol and their biological activities. *J Phys Conf Ser.* 2019; 1294(5): 052043. IOP Publishing. <https://doi.org/10.1088/1742-6596/1294/5/052043>
 - Jaber SA, Kyhoiesh HA, Jawad SH. Synthesis, characterization and biological activity studies of cadmium (II) complex derived from azo ligand 2-[2\-(5-bromo Thiazolyl) azo]-5-dimethyl amino benzoic acid. *J Phys Conf Ser.* 2021; 1818(1): 012013. <https://doi.org/10.1088/1742-6596/1818/1/012013>
 - Dahi MA, Jarad AJ. Synthesis, characterization and biological evaluation of thiazolyl azo ligand complexes with some metal ions. *J Phys Conf Ser.* 2020; 1664(1): 012090. <https://doi.org/10.1088/1742-6596/1664/1/012090>
 - Mohamed MG, EL-Mahdy AF, Kotp MG, Kuo SW. Advances in porous organic polymers: Syntheses, structures, and diverse applications. *Mater Adv.* 2022; 3(2): 707-33. <https://doi.org/10.1039/D1MA00771H>
 - Alhakimi AN, Shakdofa MM, Saeed S, Shakdofa AM, Al-Fakeh MS, Abdu AM, et al. Transition Metal Complexes Derived from 2-hydroxy-4-(p-tolyldiazenyl) benzylidene)-2-(p-tolylamino) acetohydrazide Synthesis, Structural Characterization, and Biological Activities. *J Korean Chem Soc.* 2021; 65(2): 93-105. <https://doi.org/10.5012/jkcs.2021.65.2.93>
 - Al-Hamdani AAS, Al-Alwany TAM, Mseer MA, Fadhel AM, Al-Khafaji YF. Synthesis, Characterization, Spectroscopic, Thermal and Biological Studies for New Complexes with N1, N2-bis (3-hydroxyphenyl) Oxalamide. *Egypt J Chem.* 2023; 66(4): 223-235. <https://doi.org/10.21608/EJCHEM.2022.144403.6297>
 - Kyhoiesh HA, Al-Adilee KJ. Synthesis, spectral characterization, antimicrobial evaluation studies and cytotoxic activity of some transition metal complexes with tridentate (N, N, O) donor azo dye ligand. *Results Chem.* 2021; 3: 100245. <https://doi.org/10.1016/j.rechem.2021.100245>
 - Jain S, Dongare K, Nallamotheu B, Dora CP, Kushwah V, Katiyar SS, et al. Enhanced stability and oral bioavailability of erlotinib by solid self nano emulsifying drug delivery systems. *Int J Pharm.* 2022; 622: 121852. <https://doi.org/10.1016/j.ijpharm.2022.121852>
 - Asim N, Amin MH, Alghoul MA, Sulaiman SN, Razali H, Akhtaruzzaman M *et al.* Developing of chemically treated waste biomass adsorbent for dye removal. *J Nat Fibers.* 2021; 18(7): 968-77. <https://doi.org/10.1080/15440478.2019.1675214>

25. Abdallah SM. Metal complexes of azo compounds derived from 4-acetamidophenol and substituted aniline. *Arab J Chem*. 2012 Apr 1; 5(2): 251-6. <http://doi.org/10.1016/j.arabjc.2010.08.019>.
26. Abdulridab M Q, Al-Hamdani A A S, Hussien IA. Synthesis, Characterization and Antioxidant Activity of New Azo Ligand and Some Metal Complexes of Tryptamine Derivatives. *Baghdad Sci J*. 2023; 20(3 suppl.): 1046-1063. <https://doi.org/10.21123/bsj.2023.8227>
27. Hasan M. Synthesis, Identification, and Biological Study for Some Complexes of Azo Dye Having Theophylline. *Sci World J*. 2021; 76(3): 1-9. <https://doi.org/10.1155/2021/9943763>
28. Emam SM, Abouel Enein SA, Abouzayed FI. Synthesis, spectral characterization, thermal studies and biological activity of (Z)-5-((1, 5-dimethyl-3-oxo-2-phenyl-2, 3-dihydro-1H-pyrazol-4-yl) diazenyl)-6-hydroxy-2-mercaptopyrimidin-4 (3H)-one and its metal complexes. *Appl Organomet Chem*. 2018; 32(5): e4073. <https://doi.org/10.1002/aoc.4073>
29. Al-Daffay RK, Al-Hamdani AA. Synthesis, Characterization, and Thermal Analysis of a New Acidicazo Ligand's Metal Complexes. *Baghdad Sci J*. 2023 Feb 1; 20(1): 0121-122. <https://doi.org/10.37398/JSR.2021.650206>
30. Sukeda N, Fujigaki H, Ando T, Ando H, Yamamoto Y, Saito K. Identification of 2',4',6'-Trihydroxyacetophenone as Promising Cysteine Conjugate Beta-Lyase Inhibitor for Preventing Cisplatin-Induced Nephrotoxicity. *Mol Cancer Ther*. 2023 Jun 7: OF1-OF9. <https://doi.org/10.1158/1535-7163.MCT-22-0564>.
31. Ikechukwu PE, Peter AA., Synthesis, Characterization, Anticancer, and Antioxidant Studies of Ru(III) Complexes of Monobasic Tridentate Schiff Bases. *Bioinorg Chem Appl*. 2016; (9672451): 1-11. <http://dx.doi.org/10.1155/2016/9672451>
32. Ashrafuzzaman MD, Camellia FK, Mahmud AA, Pramanik MD, Nahar K, HAQUE M. Bioactive mixed ligand metal complexes of Cu (II), Ni (II), and Zn (II) ions: synthesis, characterization, antimicrobial and antioxidant properties. *JCCHEMS*. 2021 Sep;66(3):5295-9. <http://dx.doi.org/10.4067/S0717-97072021000305295>
33. Ejidike IP, Ajibade PA. Synthesis, characterization, antioxidant, and antibacterial studies of some metal (II) complexes of tetradentate schiff base ligand:(4E)-4-[(2-(E)-[1-(2, 4-dihydroxyphenyl) ethylidene] amino ethyl) imino] pentan-2-one. *Bioinorg Chem Appl*. 2015; 890734: 1-9. <https://doi.org/10.1155/2015/890734>
34. Geary WJ. The use of conductivity measurements in organic solvents for the characterisation of coordination compounds. *Coord Chem Rev*. 1971; 7(1): 81-122. [https://doi.org/10.1016/S0010-8545\(00\)80009-0](https://doi.org/10.1016/S0010-8545(00)80009-0).
35. El-Gammal OA, Mohamed FS, Rezk GN, El-Bindary AA. Synthesis, characterization, catalytic, DNA binding and antibacterial activities of Co (II), Ni (II) and Cu (II) complexes with new Schiff base ligand. *J Mol Liq*. 2021; 326: 115223. <https://doi.org/10.1016/j.molliq.2020.115223>
36. El-Gammal OA, El-Bindary AA, Mohamed FS, Rezk GN, El-Bindary MA. Synthesis, characterization, design, molecular docking, anti COVID-19 activity, DFT calculations of novel Schiff base with some transition metal complexes. *J Mol Liq*. 2022; 346: 117850. <https://doi.org/10.1016/j.molliq.2021.117850>
37. Khedr AM, El-Ghamry H, Kassem MA, Saad FA, El-Guesmi N. Novel series of nanosized mono- and homobi-nuclear metal complexes of sulfathiazole azo dye ligand: Synthesis, characterization, DNA-binding affinity, and anticancer activity. *Inorg Chem Commun*. 2019 Oct 1; 108: 107496. <https://doi.org/10.1016/j.inoche.2019.107496>
38. Al-Atbi HS, Al-Salami BK, Al-Assadi IJ. New azo-azomethine derivative of sulfanilamide: Synthesis, Characterization, Spectroscopic, Antimicrobial and Antioxidant activity study. *J Phys: Conf Ser*. 2019; 1294(5): 052033. <https://doi.org/10.1088/1742-6596/1294/5/052033>
39. Gaikwad KD, Khobragade RM, Deodware SA, Ubale PA, Dhale PC, Ovhal RM et al. Chemical synthesis, spectral characterization and biological activities of new diphenylsulphone derived Schiff base ligand and their Ni (II) complexes. *Results Chem*. 2022 Jan 1; 4: 100617. <https://doi.org/10.1016/j.rechem.2022.100617>
40. Vhanale B, Kadam D, Shinde A. Synthesis, spectral studies, antioxidant and antibacterial evaluation of aromatic nitro and halogenated tetradentate Schiff bases. *Heliyon*. 2022 Jun 1; 8(6): 09650. <https://doi.org/10.1016/j.heliyon.2022.e09650>.

تحضير, تشخيص ودراسة حرارية لمعقدات Au (III) و Cd(II), Zn(II), Cu(II), VO(II) معليكاند صبغة الأزو وتقييمها كمضادات أكسدة

اريج ملك فاضل¹, عباس علي صالح الحمداني², وائل الزغبى³

¹وزارة التربية, مديرية تربية بغداد الرصافة الثانية.

²قسم الكيمياء, كلية العلوم للبنات, جامعة بغداد, بغداد, العراق.

³مجموعة الكيمياء الكهربائية للمواد, كلية علوم وهندسة المواد, جامعة يونسجام, جيونجسان, جمهورية كوريا.

الخلاصة

حضرت معقدات كل من الفنادايل, الخارصين, النحاس والكادميوم بتكافؤهم الثنائي والذهب بتكافؤه الثلاثي باستخدام صبغة ازوجديدة (2,4,6-ثلاثي هيدروكسي-3-((3-هيدروكسي فنيل) ثنائي زينيل) فنيل) ايثان-1-اون المحضرة من ملح الديازونيوم مع 2,4,6- ثلاثي هيدروكسي اسيتوفينون بعد عزل (E)-1-(2,4,6-trihydroxy-3-((3-hydroxyphenyl)diazanyl)phenyl)ethan-1-one تم تشخيصها بواسطة الطرق الطيفية المتاحة والتقنيات التشخيصية لكل من التحليل الدقيق للعناصر واطياف كل من الكتلة, الرنين النووي البروتوني والكاربوني, الاشعة فوق البنفسجية, الاشعة تحت الحمراء ومنحنى التحلل الحراري الوزني والمسعر التفاضلي والمعقدات شملت التقنيات هذه فضلا عن تحديد نسبة الفلز وتحديد محتوى الكلور والحساسية المغناطيسية والتوصيلية المولارية. أعطت النتائج أن الليكاند ايوني (سالب) رباعي السن مرة عند تناسقه مع النحاس والخارصين والكادميوم عن طريق ذرة الاوكسجين الفينولية و ذرة الاوكسجين الكاربونيلية وذرة نتروجين الأزو, بينما كان ثلاثي السن عند التناسق مع الذهب الثلاثي من خلال ذرة الاوكسجين الفينولية وذرة نتروجين الأزو حيث اعطى الذهب شكل مربع مستوي متعادل بينما الخارصين والكادميوم ثنائي السطوح متعادل حاوي على جزيئين ماء متناسقة واعطى النحاس شكل رباعي السطوح متعادل اما الفنادايل فاعطى شكلا ثنائي الهرم المثلي متعادل. ثم تم تحديد قابلية هذه المركبات المحضرة كمضادات اكسدة من خلال كبحها للجذور الحرة باستعمال مادة DPPH كجذر حر وفيتامين C كمرجع لتحديد قيمة IC₅₀ التي اعطت النتائج (Au-complex > H₄L > Ascorbic acid > Zn-complex > Cu-complex > Cd-complex > V-complex)

الكلمات المفتاحية: معقدات الأزو، أصباغ الأزو، تأثير مضادات الاكسدة، التحليل الحراري الوزني، 2,4,6-هيدروكسي اسيتوفينون.